



11 W continuous-wave laser operation at 2.09 μm in $\text{Tm}:\text{Lu}_{1.6}\text{Sc}_{0.4}\text{O}_3$ mixed sesquioxide ceramics pumped by a 796 nm laser diode

ZHENDONG HAO,^{1,2} LIANGLIANG ZHANG,^{1,2} YUNPENG WANG,¹ HAO WU,¹ GUO-HUI PAN,¹ HUAJUN WU,¹ XIA ZHANG,¹ DONGXU ZHAO,¹ AND JIAHUA ZHANG^{1,*}

¹State Key Laboratory of Luminescence and Applications, Changchun Institute of Optics, Fine Mechanics and Physics, Chinese Academy of Sciences, Changchun 130033, China

²These authors contribute equally to this work

*zhangjh@ciomp.ac.cn

Abstract: High quality thulium doped $\text{Lu}_{1.6}\text{Sc}_{0.4}\text{O}_3$ mixed sesquioxide laser ceramics were fabricated using a solid-state reactive sintering method. Optical and spectroscopic properties of the ceramics were studied. A high transmittance almost identical to the theoretical value of the ceramics was reached at the lasing wavelength. A large Stark splitting of 920 cm^{-1} for the ground states $^3\text{H}_6$ and 472 cm^{-1} for the first excited states $^3\text{F}_4$ of Tm^{3+} were observed, resulting in a long wavelength emission band around $2.09\text{ }\mu\text{m}$ with low reabsorption losses at this wavelength. CW laser operation at $2.09\text{ }\mu\text{m}$ pumped by a 796 nm laser diode was achieved with an output power of 11 W and an optical-to-optical conversion efficiency of 28.9%, both of which are the highest values reported so far for lasing around $2.1\text{ }\mu\text{m}$ in Tm^{3+} doped mixed sesquioxide ceramics.

© 2018 Optical Society of America under the terms of the [OSA Open Access Publishing Agreement](#)

1. Introduction

Solid state lasers operating around $2\text{ }\mu\text{m}$ are of great interest for many applications, such as medicine, environment monitoring and lidar systems [1]. The wavelengths above $2\text{ }\mu\text{m}$ are suitable for pumping ZnGeP_2 (ZGP) optical parametric oscillators to efficiently generate 3-5 μm mid-infrared radiation via non-linear frequency conversion [2]. Holmium lasers reach longer wavelengths such as $2.09\text{ }\mu\text{m}$ in $\text{Ho}:\text{YAG}$ [3–5]. The pump wavelength required for Ho^{3+} lasers is $1.9\text{ }\mu\text{m}$, for which the high power pumping laser diodes (LD) are commercially unavailable. The Ho^{3+} lasers are directly pumped by a $\text{Tm}:\text{YLF}$ laser (pumped by a 796 nm LD), where the lasing around $1.9\text{ }\mu\text{m}$ is the transition from the first excited state $^3\text{F}_4$ to the ground state $^3\text{H}_6$ of Tm^{3+} .

Rare earth sesquioxides have a high thermal conductivity compared with YAG [6]. Fortunately, Tm^{3+} doped rare earth sesquioxides [7–9], Lu_2O_3 and Sc_2O_3 , show very large Stark splittings in the ground state manifolds due to the strong crystal field strength in the sesquioxides, enabling the $^3\text{F}_4$ - $^3\text{H}_6$ transition to produce a long wavelength emission band around $2.1\text{ }\mu\text{m}$. The $^3\text{F}_4$ state can be populated upon $^3\text{H}_4$ excitation around 800 nm through cross relaxation with a neighboring Tm^{3+} in the ground state, resulting in quantum conversion of one 800 nm photon into two $2.1\text{ }\mu\text{m}$ photons [10]. The unique optical properties of Tm^{3+} doped sesquioxides enable lasing around $2.1\text{ }\mu\text{m}$ to be directly generated by 800 nm LD pump with the theoretical limit for the slope conversion efficiency to 76%. Koopmann and associates [7–9] reported, for the first time, continuous-wave (CW) laser operation at $2.065\text{ }\mu\text{m}$ in $\text{Tm}^{3+}:\text{Lu}_2\text{O}_3$ and $2.116\text{ }\mu\text{m}$ in $\text{Tm}^{3+}:\text{Sc}_2\text{O}_3$ single crystals pumped by a 800 nm LD. An output power of 75 W and the slope efficiency of 40% were achieved in $\text{Tm}:\text{Lu}_2\text{O}_3$ [7], indicating Tm^{3+} doped sesquioxides could become an alternative to $\text{Ho}:\text{YAG}$ lasers. These sesquioxide single crystals, however, are difficult to produce due to a high melting

temperature (~ 2450 °C) [8]. Sintering of sesquioxide transparent ceramics has, therefore, attracted tremendous attention because the sintering temperature is much lower than the melting temperature [11,12]. Antipov and associates realized significant CW laser operation at $2.068 \mu\text{m}$ of $\text{Tm}^{3+}:\text{Lu}_2\text{O}_3$ ceramics pumped by 800 nm LDs [13–15]. An output power of 34 W with a slope efficiency of 44% were achieved [15].

Compared with $\text{Tm}^{3+}:\text{Lu}_2\text{O}_3$, $\text{Tm}^{3+}:(\text{Lu},\text{Sc})_2\text{O}_3$ mixed crystals can reach a longer emission wavelength [16], which is beneficial for efficient generation of mid-infrared radiation via pumping ZGP. Meanwhile, the mixed crystals provide a disordered crystal structure and thus inhomogeneously broadened optical spectra of Tm^{3+} compared with Tm^{3+} in Lu_2O_3 single crystals [16]. The inhomogeneous broadening can compress the pulse width in mode-locked operation on one hand and improve the matching of the absorption band with the pump laser wavelength on the other hand. Very recently, CW laser operations around $2 \mu\text{m}$ in some Tm^{3+} doped mixed sesquioxide ceramics pumped by 800 nm LDs were reported [17–19].

Xu et al. reported 211 mW lasing at $1.92 \mu\text{m}$ in $\text{Tm}:\text{LuScO}_3$ ceramics with the slope efficiency of 8.2% [17]. Jing et al. reported 1 W lasing at $2.1 \mu\text{m}$ in a microchip $\text{Tm}:(\text{Lu}_{2/3}\text{Sc}_{1/3})_2\text{O}_3$ ceramic with the slope efficiency of 24% [18]. Zhou reported 1.55 W lasing at $2.05 \mu\text{m}$ in $\text{Tm}:\text{LuYO}_3$ ceramics with the slope efficiency of 19.9% [19]. With the consideration of achievement of a lasing wavelength of Tm^{3+} longer than that in Lu_2O_3 , the selection of $(\text{Lu},\text{Sc})_2\text{O}_3$ mixed crystals as a host is necessary rather than $(\text{Lu},\text{Y})_2\text{O}_3$. In the reported $\text{Tm}:(\text{Lu},\text{Sc})_2\text{O}_3$ mixed ceramics [17,18], the Sc/Lu compositions ratio are 1/1 and 1/2. A smaller Sc/Lu ratio has not been studied for evaluating its lasing performance.

In this paper, we report optical properties and 796 nm LD pumped 11 W CW lasing at $2.09 \mu\text{m}$ with 28.9% optical-to-optical conversion efficiency in Tm^{3+} doped $\text{Lu}_{1.6}\text{Sc}_{0.4}\text{O}_3$ mixed ceramics with the Sc/Lu ratio of 1/4.

2. Description of experiment

The ceramics of this work were fabricated in our lab using a solid-state reactive sintering method. Lu_2O_3 , Sc_2O_3 and Tm_2O_3 (5 N) powders were used as the starting materials. ZrO_2 (99.5%) powder was used as a sintering aid. For fabrication of 1% $\text{Tm}:\text{Lu}_{1.6}\text{Sc}_{0.4}\text{O}_3$ and 1.5% $\text{Tm}:\text{Lu}_{1.6}\text{Sc}_{0.4}\text{O}_3$ ceramics, the raw materials were weighted with stoichiometric compositions of $0.99(0.8\text{Lu}_2\text{O}_3-0.2\text{Sc}_2\text{O}_3)-0.01\text{Tm}_2\text{O}_3$ and $0.985(0.8\text{Lu}_2\text{O}_3-0.2\text{Sc}_2\text{O}_3)-0.015\text{Tm}_2\text{O}_3$, respectively. In addition, the sintering aid was added with 3.0 wt%. The weighted powders were then milled in ethanol with zirconia balls for 48 h by a planetary ball-mill (RETSCH PM400, Germany). The ethanol solvent is removed by drying the milled slurry at 60 °C for 24 h and uniform granules are made by sieving through a 200 mesh screen. These sieved powders were calcined at 800 °C for 10 h and pressed into square plate shaped green bodies with a $20 \times 25 \text{ mm}^2$ square stainless steel mold at 10 MPa and then cold isostatically pressed at 200 MPa. The green bodies were pre-sintered at 1800 °C for 15 h in vacuum ($\sim 10^{-3}$ Pa) for densification and then post-sintered by Hot Isostatic Pressing (HIP) for further densification at 1700 °C for 2 h in argon gas with gas pressure of 200 MPa. Finally, the sintered ceramics were annealed at 1500 °C for 10 h in air to eliminate the oxygen vacancies and remove internal stresses. Highly transparent ceramics can be achieved after optical polishing. After cutting, the square plate ceramics with the sizes of $2.6 \times 15 \times 18 \text{ mm}^3$ are obtained for the study of optical properties, and the rectangular bars with the size of $2.6 \times 2.6 \times 15 \text{ mm}^3$ for laser operation experiments.

The polycrystalline phase of the samples was analyzed by X-ray diffraction (XRD) (D8 Focus, Bruker, Germany) using $\text{Cu K}\alpha$ radiation. The morphology of the polished ceramic surface was characterized by field emission scanning electron microscopy (FE-SEM, Hitachi, S-4800). The optical transmission spectra were measured using a UV-VIS-NIR spectrometer (UV-3600plus, Shimadzu, Japan). The infrared emission spectra were recorded by a fiber optics optical meter (Ocean Optical, NIRQUEST256-2.5) under excitation of 800 nm LD.

The samples were placed in a temperature controlled microscope stage (Linkam-THM S600, UK).

3. Results and discussion

The SEM morphologies of the thermal etching surface of the ceramics display pore-free patterns, as shown in Fig. 1(a). The grain boundaries are clean and no abnormal grains is observed. The average grain size is $1.54 \mu\text{m}$. Figure 1(b) shows the XRD pattern of 1.5% Tm: $\text{Lu}_{1.6}\text{Sc}_{0.4}\text{O}_3$ ceramic together with the standard patterns of cubic Lu_2O_3 (JPCD cards. 12-0728) and Sc_2O_3 (JPCD cards. 74-1210) for comparison. The measured pattern shows the identical structure to the standard patterns except the shift of diffraction angles, indicating pure cubic phase of the mixed sesquioxide ceramic. The XRD peaks of the ceramic are located between that of Lu_2O_3 and Sc_2O_3 , reflecting the existence of Lu_2O_3 - Sc_2O_3 solid solution.

Figure 1(c) illustrates the transmission spectrum for 1.5% Tm: $\text{Lu}_{1.6}\text{Sc}_{0.4}\text{O}_3$ ceramic plate with a thickness of 2.6 mm. A series characteristic absorption bands of Tm^{3+} appear in the range of 500 – 2300 nm, responsible for the transitions from the ground state $^3\text{H}_6$ to the excited states $^3\text{F}_{2,3}$, $^3\text{H}_4$, $^3\text{H}_5$ and $^3\text{F}_4$. High transmittances appear outside of the Tm^{3+} absorption bands. The transmittance at the lasing wavelength of $2.09 \mu\text{m}$ reaches 82.21% (circle), much close to the theoretical value (brackets) of 82.28% calculated by the modified Fresnel equation [20] $T = 2n/(n^2 + 1)$, with n the refractive index of the ceramic. Using the refractive indices of 1.896 for Lu_2O_3 and 1.946 for Sc_2O_3 at $2 \mu\text{m}$, we can determine the refractive index of the mixed ceramic to be 1.906 around $2 \mu\text{m}$ if assuming a linear dependence of n on the composition in the $0.8\text{Lu}_2\text{O}_3$ - $0.2\text{Sc}_2\text{O}_3$ solid solution.

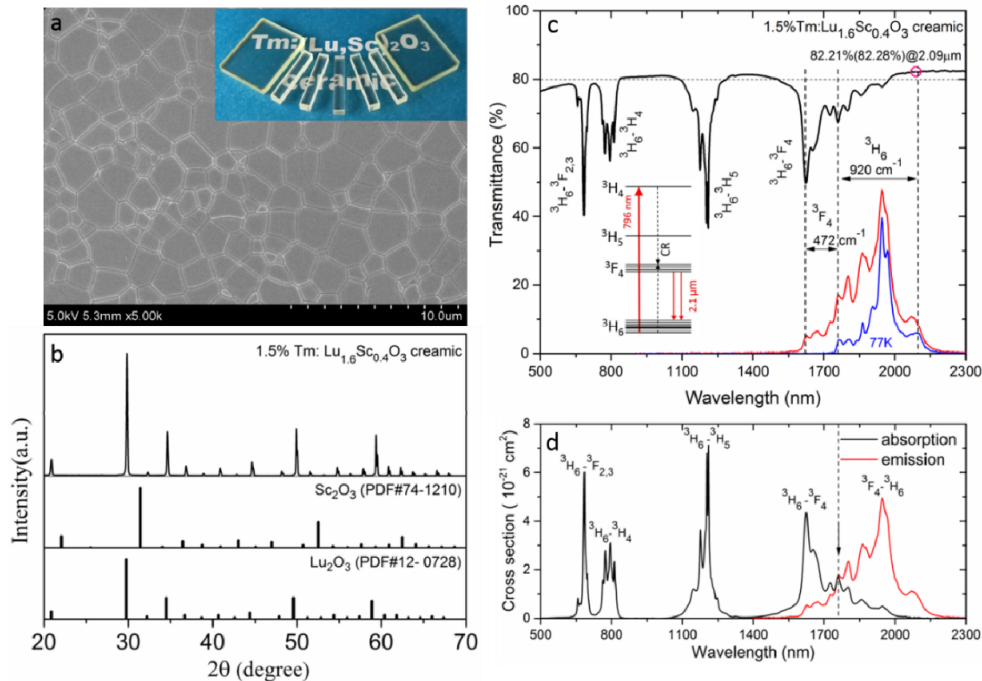


Fig. 1. Characterization of 1.5% Tm: $\text{Lu}_{1.6}\text{Sc}_{0.4}\text{O}_3$ ceramic. a: SEM morphology of the thermal etching surface and a inserted photo of a ceramic square plate ($2.6 \times 15 \times 18 \text{ mm}^3$) with 5 rectangular bars ($2.6 \times 2.6 \times 15 \text{ mm}^3$). b: XRD patterns. c: Transmission and emission spectra with an energy level diagram showing cross relaxation (CR) between two Er^{3+} ions and $2.1 \mu\text{m}$ emissions due to a large Stark splitting of the $^3\text{H}_6$ ground states. d: The stimulated emission and absorption cross sections.

The 3F_4 - 3H_6 emission spectra are measured at room temperature (RT) and 77 K, respectively, upon 3H_4 excitation at 796 nm, as shown in Fig. 1(c). The 77 K spectrum covers a spectral range narrower than the RT one. At low temperature of 77 K the 3F_4 populations are considered to almost occupy the lowest Stark level of the 3F_4 manifold and the emission is contributed by the transition from the lowest Stark level of 3F_4 to the 3H_6 manifold. Hence, the spectral distribution range of the 77K emission reflects the Stark splitting of the 3H_6 manifold. In the 77K emission spectrum the emission peaks cover from 1760 to 2100 nm, indicating a 920 cm^{-1} Stark splitting of the 3H_6 manifold with the transition peak between the lowest Stark levels of the 3F_4 and the 3H_6 states at 1760 nm. In the RT emission spectrum some additional emission peaks appear in the high energy side of the 77K emission, ranging from 1625 to 1760 nm. These additional emissions are attributed to the transitions from the upper Stark levels of 3F_4 , which can be populated thermally as the temperature is raised from 77K to RT. As a result, the distribution range of these additional peaks indicates the range of Stark splitting of the 3F_4 states, which is 472 cm^{-1} for the energy separation between 1625 and 1760 nm. Obviously, the large Stark splitting of the 3H_6 and 3F_4 states enable the 3F_4 - 3H_6 emission to contain a long wavelength emission band around $2.09\text{ }\mu\text{m}$, originated from the transition from the lowest Stark level of 3F_4 to the highest Stark level of 3H_6 , as illustrated in the energy level diagram of Tm^{3+} in Fig. 1(c). Moreover, the large Stark splitting of 3H_6 also results in low reabsorption losses around $2.09\text{ }\mu\text{m}$, being favorite of laser operation. The cross-sections of the stimulated emission and the absorption are plotted together as shown in Fig. 1(d), wherein the cross-section of the emission is scaled to that of absorption for the transition (arrowed) between the lowest stark levels of the 3F_4 and the 3H_6 manifolds according to the results for Tm^{3+} doped $(\text{Lu,Sc})_2\text{O}_3$ reported previously by Kränkel [21] and Jing [18]. One can see that the stimulated emission cross section at $2.09\text{ }\mu\text{m}$ is $1.1 \times 10^{-21}\text{ cm}^2$ and the absorption cross section at 796 nm responsible for 3H_6 - 3H_4 transition is $3.1 \times 10^{-21}\text{ cm}^2$.

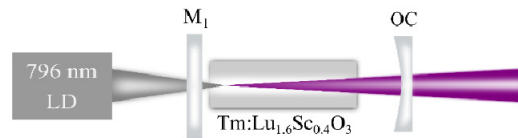


Fig. 2. Schematic of the ceramic laser setup with a cavity formed by an incoupling mirror (M1) and an output coupler (OC) pumped by a 796 nm laser diode.

The laser experimental setup is schematically shown in Fig. 2. The pump source was a fiber-coupled 796 nm AlGaAs diode laser (LIMO, Germany). A two-lens telescope with a magnification of 1:2 was used for image transfer of a pump beam from a $400\text{-}\mu\text{m}$ fiber output into the ceramic bars. The incoupling mirror (M1) had a high transmission at 796 nm and high reflection at 2090 nm. The output coupler (OC) was partially transmitting at 2090 nm and highly reflective at 796 nm, leading to a double pass of the pump radiation through the ceramic laser bars. The cavity length is 100 mm. The OC had a transmission of 2.3% at 2090 nm and a curvature radius of 120 mm. $\text{Tm: Lu}_{1.6}\text{Sc}_{0.4}\text{O}_3$ (1 or 1.5 at.% of Tm^{3+}) ceramic bars with the sizes of $2.6 \times 2.6 \times 15\text{ mm}^3$ were used. Both facets in all the bars had an antireflective coating for the pump and lasing wavelengths at 796 nm and 2090 nm, respectively. The ceramic bars were wrapped with indium foil and fixed in a Cu radiator. The temperature of the radiator was stabilized by external water.

The gain cross-section, which can be calculated by [18]

$$\sigma_g = \beta\sigma_{SE} - (1-\beta)\sigma_{abs} \quad (1)$$

where σ_g , σ_{SE} and σ_{abs} are the cross sections of gain, stimulated emission and absorption, respectively; β is the inversion ratio, defined as the population ratio of the 3F_4 to the 3H_6 . Using the spectral data for the σ_{SE} and σ_{abs} shown in Fig. 1d, the gain cross-sections for various β are obtained from Eq. (1), as shown in Fig. 3a. One can see that the gain appears the

maximum around 2090 nm for β less than 0.06. Figure 3(b) shows the output laser spectrum peaking at 2090 nm, the center of the gain curve.

Figure 3(c) depicts the pump power dependence of output power for 1% Tm^{3+} and 1.5% Tm^{3+} doped $\text{Lu}_{1.6}\text{Sc}_{0.4}\text{O}_3$ ceramics. The corresponding optical-to-optical conversion efficiencies are shown in Fig. 3(d). An output power of 9.8 W is reached under 38 W pump for the 1% Tm^{3+} ceramic, indicating an optical-to-optical conversion efficiency of 25.8%. In the 1.5% Tm^{3+} ceramic, an 11 W output with 28.9% conversion efficiency under 38 W pump were achieved. One can also see that the slope efficiencies are 34.4% and 37.1% with respect to the pump power for 1% Tm^{3+} and 1.5% Tm^{3+} , respectively. Since the ceramic absorbed approximately 85% of the pump light for 1% Tm^{3+} , and 95% for 1.5% Tm^{3+} , the corresponding slope efficiencies with respect to the absorbed pump power are about 40% and 39%, which are both larger than the theoretical limit (38%) for the conversion from one 796 nm photon to one 2090 nm photon. As a result, the cross relaxation between two Tm^{3+} ions for converting one 796 nm photon to two 2090 nm photons made a contribution to $^3\text{F}_4$ population. The observation of the cross relaxation effect indicates a high quality of the laser ceramics sintered in this work that the depletion of the population of the pump level $^3\text{H}_4$ through defects is suppressed. These output powers and efficiencies obtained in this work are the highest values reported so far for lasing around 2.1 μm in Tm^{3+} doped mixed sesquioxide ceramics pumped by a 796 nm diode. As the pump power is higher than 30 W, the deviation of the output power from the linear dependence is observed for both the ceramics. We attribute the phenomenon to thermal effect. The optimization of Tm^{3+} concentration and the ceramic length is necessary in the future study. The results of this work indicate that Tm^{3+} doped rare-earth mixed sesquioxide ceramics is a promising solid laser medium for 2.1 μm laser operation pumped by a 796 nm laser diode.

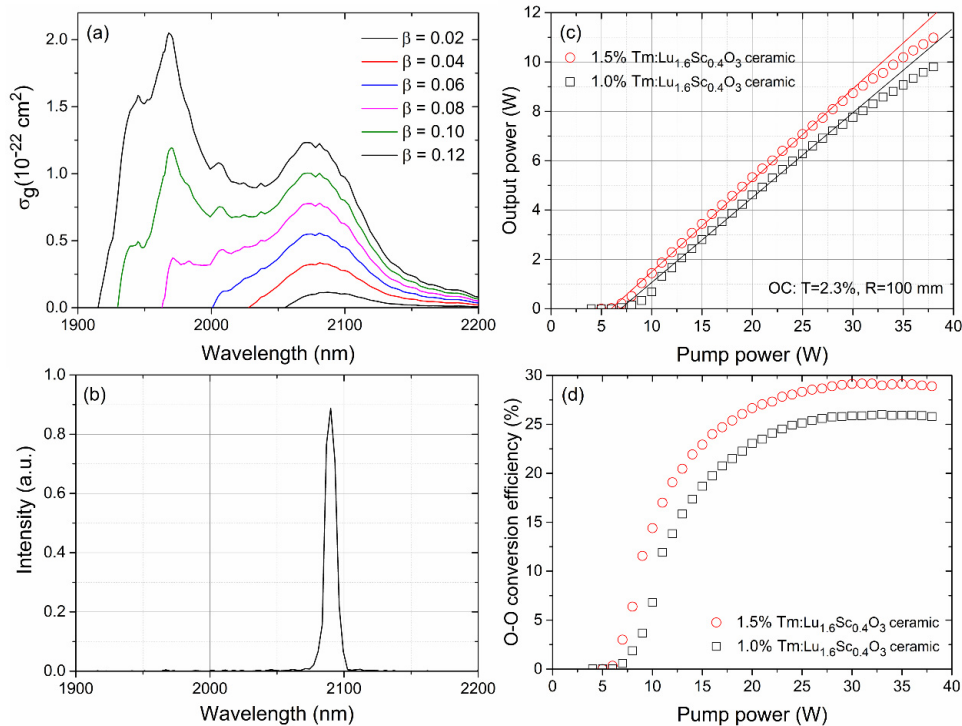


Fig. 3. The gain cross sections (a) and output laser spectrum (b) of 1.5% Tm^{3+} : $\text{Lu}_{1.6}\text{Sc}_{0.4}\text{O}_3$ ceramic. The pump power dependence of output power (c) and optical-to-optical conversion efficiencies (d) for 1% Tm^{3+} and 1.5% Tm^{3+} doped $\text{Lu}_{1.6}\text{Sc}_{0.4}\text{O}_3$ ceramics.

4. Summary

Highly transparent $\text{Lu}_{1.6}\text{Sc}_{0.4}\text{O}_3$ mixed sesquioxide ceramics doped with 1% Tm^{3+} or 1.5% Tm^{3+} has been fabricated by using a solid-state reactive sintering method, namely, pre-sintered in vacuum and then post-sintered by HIP. The polycrystalline ceramics consists of small grains with an average size of 1.54 μm . The transmittance at 2.09 μm reaches 82.21%, nearing the theoretical value of 82.28% at 2 μm . Large Stark splittings of 920 cm^{-1} in the ground state $^3\text{H}_6$ manifold and 472 cm^{-1} in the $^3\text{F}_4$ of Tm^{3+} are observed and they result in a long wavelength emission band around 2.09 μm due to transition from the lowest Stark level $^3\text{F}_4$ to the highest Stark level of $^3\text{H}_6$. The large Stark splitting of the ground states also minimize the reabsorption losses at 2.09 μm , making efficient and high power lasing at this wavelength possible. 11 W CW laser operation at 2.09 μm with an optical-to-optical conversion efficiency of 28.9% was achieved in 1.5% $\text{Tm}:\text{Lu}_{1.6}\text{Sc}_{0.4}\text{O}_3$ mixed ceramic pumped by a 796 nm LD, exhibiting its attractive application prospect.

Funding

The innovation program of CIOMP, National Natural Science Foundation of China (51772286, 11874055, 11604330) and National Key R&D Program of China (2016YFB0701003, 2016YFB0400605). Natural Science Foundation of Jilin province (20160520171JH).

References

1. K. Scholle, S. Lamrini, P. Koopmann, and P. Fuhrberg, "2 mm Laser Sources and Their Possible Applications," in *Frontiers in Guided Wave Optics and Optoelectronics*, E. D. Bishnu Pal, ed. (INTECH, 2010)
2. A. Hemming, J. Richards, A. Davidson, N. Carmody, S. Bennetts, N. Simakov, and J. Haub, "99 W mid-IR operation of a ZGP OPO at 25% duty cycle," *Opt. Express* **21**(8), 10062–10069 (2013).
3. P. A. Budni, L. A. Pomeranz, M. L. Lemons, C. A. Miller, J. R. Mosto, and E. P. Chicklis, "Efficient midinfrared laser using 1.9- μm -pumped Ho:YAG and ZnGeP₂ optical parametric oscillators," *J. Opt. Soc. Am. B* **17**(5), 723–728 (2000).
4. Y. J. Shen, B. Q. Yao, X. M. Duan, T. Y. Dai, Y. L. Ju, and Y. Z. Wang, "Resonantly pumped high efficiency Ho:YAG laser," *Appl. Opt.* **51**(33), 7887–7890 (2012).
5. Y. J. Shen, B. Q. Yao, X. M. Duan, G. L. Zhu, W. Wang, Y. L. Ju, and Y. Z. Wang, "103 W in-band dual-end-pumped Ho:YAG laser," *Opt. Lett.* **37**(17), 3558–3560 (2012).
6. J. Sanghera, W. Kim, G. Villalobos, B. Shaw, C. Baker, J. Frantz, B. Sadowski, and I. Aggarwal, "Ceramic laser materials," *Materials (Basel)* **5**(12), 258–277 (2012).
7. P. Koopmann, S. Lamrini, K. Scholle, P. Fuhrberg, K. Petermann, and G. Huber, "Efficient diode-pumped laser operation of $\text{Tm}:\text{Lu}_2\text{O}_3$ around 2 μm ," *Opt. Lett.* **36**(6), 948–950 (2011).
8. P. Koopmann, R. Peters, K. Petermann, and G. Huber, "Crystal growth, spectroscopy, and highly efficient laser operation of thulium-doped Lu_2O_3 around 2 μm ," *Appl. Phys. B* **102**(1), 19–24 (2011).
9. P. Koopmann, S. Lamrini, K. Scholle, P. Fuhrberg, and K. Petermann, "Long wavelength laser operation of $\text{Tm}:\text{Sc}_2\text{O}_3$ at 2116 nm and beyond," in *Advances in Optical Materials*, OSA Technical Digest (Optical Society of America, 2011), paper ATuA5.
10. A. Brenier, C. Pedrini, B. Moine, J. L. Adam, and C. Pledel, "Fluorescence mechanisms in Tm^{3+} singly doped and Tm^{3+} , Ho^{3+} doubly doped indium-based fluoride glasses," *Phys. Rev. B Condens. Matter* **41**(8), 5364–5371 (1990).
11. V. Lupei, A. Lupei, and A. Ikesue, "Single crystal and transparent ceramic Nd-doped oxide laser materials: a comparative spectroscopic investigation," *J. Alloys Compd.* **380**(1), 61–70 (2004).
12. G. A. Newburgh, A. Word-Daniels, A. Michael, L. D. Merkle, A. Ikesue, and M. Dubinskii, "Resonantly diode-pumped $\text{Ho}^{3+}:\text{Y}_2\text{O}_3$ ceramic 2.1 μm laser," *Opt. Express* **19**(4), 3604–3611 (2011).
13. O. L. Antipov, S. Y. Golovkin, O. N. Gorshkov, N. G. Zakharov, and A. P. Zinoviev, "Structural, optical, and spectroscopic properties and efficient two-micron lasing of new $\text{Tm}^{3+}:\text{Lu}_2\text{O}_3$ ceramics," *Quantum Electron.* **41**(10), 863–868 (2011).
14. O. L. Antipov, A. A. Novikov, N. G. Zakharov, and A. P. Zinoviev, "Optical properties and efficient laser oscillation at 2066 nm of novel $\text{Tm}:\text{Lu}_2\text{O}_3$ ceramics," *Opt. Mater. Express* **2**(2), 183–189 (2012).
15. O. L. Antipov, A. A. Novikov, N. G. Zakharov, A. P. Zinoviev, H. Yagi, N. V. Sakharov, M. V. Kruglova, M. O. Marychev, O. N. Gorshkov, and A. A. Lagatskii, "Efficient 2.1- μm lasers based on $\text{Tm}^{3+}:\text{Lu}_2\text{O}_3$ ceramics pumped by 800-nm laser diodes," *Phys. Status Solidi., C Curr. Top. Solid State Phys.* **10**(6), 969–973 (2013).
16. P. Koopmann, S. Lamrini, K. Scholle, P. Fuhrberg, and K. Petermann, "Laser Operation and Spectroscopic Investigations of $\text{Tm}:\text{LuScO}_3$," in *CLEO/Europe and EQEC 2011 Conference Digest*, OSA Technical Digest (Optical Society of America, 2011), paper CA1_4.

17. X. Xu, Z. Hu, D. Li, P. Liu, J. Zhang, B. Xu, and J. Xu, "First laser oscillation of diode-pumped Tm^{3+} -doped LuScO_3 mixed sesquioxide ceramic," *Opt. Express* **25**(13), 15322–15329 (2017).
18. W. Jing, P. Loiko, J. M. Serres, Y. Wang, E. Vilejshikova, M. Aguiló, F. Diaz, U. Griebner, H. Huang, V. Petrov, and X. Mateos, "Synthesis, spectroscopy, and efficient laser operation of "mixed" sesquioxide $\text{Tm}:(\text{Lu},\text{Sc})_2\text{O}_3$ transparent ceramics," *Opt. Mater. Express* **7**(11), 4192–4202 (2017).
19. Z. Zhou, X. Guan, X. Huang, B. Xu, H. Xu, Z. Cai, X. Xu, P. Liu, D. Li, J. Zhang, and J. Xu, " Tm^{3+} -doped LuYO_3 mixed sesquioxide ceramic laser: effective 2.05 μm source operating in continuous-wave and passive Q-switching regimes," *Opt. Lett.* **42**(19), 3781–3784 (2017).
20. L. B. Kong, Y. Z. Huang, W. X. Que, T. S. Zhang, and S. Li, "Transparent Ceramics," in *Topics in Mining, Metallurgy and Materials Engineering*, E. D. Carlos, P. Bergmann, ed. (Springer, 2015).
21. C. Kränkel, "High-Power Lasers in the 1-, 2-, and 3- μm Spectral Range High-Power Lasers in the 1-, 2-, and 3- μm Spectral Range," *IEEE J. Sel. Top. Quantum Electron.* **21**(1), 250–262 (2015).